Final Report under
NASA Cooperative Agreement
NCC 3-56

**MODERN DEVELOPMENTS IN SHEAR FLOW CONTROL
WITH SWIRL**

KU-FRL-724-4

S. Farokhi
and
R. Taghavi

Flight Research Laboratory
The University of Kansas Center for Research, Inc.
Lawrence, Kansas 66045-2969

May 1990

Abstract

Passive and active control of swirling turbulent jets is experimentally investigated. Initial swirl distribution is shown to dominate the free jet evolution in the passive mode. Vortex breakdown, a manifestation of high-intensity swirl, was achieved at below-critical swirl number (S = 0.48) by reducing the vortex core diameter. The response of a swirling turbulent jet to single-frequency, plane-wave acoustic excitation was shown to depend strongly on the swirl number, excitation Strouhal number, amplitude of the excitation wave, and core turbulence in a low-speed cold jet. A 10% reduction of the mean centerline velocity at x/D = 9.0 (and a corresponding increase in the shear layer momentum thickness) was achieved by large amplitude internal plane-wave acoustic excitation. Helical instability waves of negative azimuthal wave numbers exhibit larger amplification rates than the plane waves in swirling free jets, according to hydrodynamic stability theory. Consequently, an active swirling shear layer control is proposed to include the generation of helical instability waves of arbitrary helicity and the promotion of modal interaction, through multifrequency forcing.

Table of Contents

Nomenclature

A,B,C   outer, middle, and inner swirl-generating manifolds, respectively

c   constant

D   nozzle exit diameter

f   excitation frequency, Hz

G   degree of swirl, $\equiv W_{m0}/U_{m0}$

G_x axial flux of axial momentum

G_ϕ axial flux of angular momentum

M   mean axial Mach number (based on the mass-averaged axial velocity)

O   order of

P_∞ ambient pressure

p   static pressure

R   nozzle exit radius, 1.75 in (4.45 cm)

S   swirl number

st   Strouhal number

U,V,W   mean axial, radial, and tangential velocity components in the jet, respectively

U_c time-mean axial velocity component on the jet centerline

U_{ce} time-mean velocity component at the center of the nozzle exit

U_α mass-averaged axial velocity at the nozzle exit

u',v',w'   fluctuating axial, radial, and tangential velocity components in the jet, respectively

u'_c rms axial velocity fluctuation on the jet centerline

u'_f fundamental rms amplitude

u'_{fe} fundamental rms amplitude at the center of the nozzle exit

x   axial distance from the nozzle exit plane along the jet centerline

x,r,ϕ cylindrical polar coordinates in the jet

ε   very small quantity

θ   momentum thickness (in)

ρ   fluid density

Subscripts:

crit   critical

m   maximum

x   quantity along the jet centerline

0   initial value (i.e., condition at

          $x/D = 0$)

∞   unperturbed, ambient condition

Abbreviations:

dB   decibel (re. 20 μPa)

SPL   sound pressure level

1. Introduction and Review of Literature

Turbulent shear layers with swirl exhibit distinctive characters absent in their non-rotating counterparts. A subsonic swirl-free jet, for example, experiences theoretically no static pressure gradient in the axial or radial direction. Hence, in this case, the mechanism for jet spread is dominated by the turbulent mixing at the interface between the jet and the ambient fluid. On the other hand, a turbulent jet with strong swirl is primarily driven in the near field (x/D < 5) by the static pressure gradients in both axial and radial directions, i.e. mainly an inviscid phenomenon. Turbulent mixing then becomes a dominant factor only when the strong pressure gradients are weakened through rapid initial jet spread (i.e. a jet in near pressure equilibrium). The absence of potential core in a swirling jet is, by definition, another feature which distinguishes the rotating from the nonrotating jets.

The nondimensional parameter describing the integrated swirl strength in a jet is the swirl number S, and is defined as

$$S \equiv G_\phi / G_x R \tag{1}$$

where the jet torque is

$$G_\phi \equiv 2\pi \int_0^\infty \rho U W r^2 dr \tag{2}$$

the jet axial thrust is

$$G_x \equiv 2\pi \int_0^\infty [\rho U^2 + (p - p_\infty)] r \, dr \tag{3}$$

and R is the nozzle exit radius. By definition, the swirl number is an integrated quantity; hence, it is possible to generate swirling jets with different initial tangential velocity profiles ranging from solid-body rotation [i.e., $W_0(r) = c \cdot r$] to near free-vortex flow [i.e., $W_0(r) \approx c/r$] with constant S. Moreover, since the static pressure field is coupled to the

tangential velocity distribution through the momentum equations and dominates the swirling jet evolution in the near field, vastly different mean jet behavior (e.g., mean centerline velocity decay) should be observable in swirling jets with constant S. The use of variable initial tangential velocity distribution as a means of controlling the mixing characteristics of a turbulent swirling jet constitutes a _passive_ control which the authors experimentally investigated in Ref. 1. Further discussion on this research is left for the section on results.

The evolution of a subsonic swirling turbulent jet issuing from a nozzle into ambient fluid depends on the _method_ of swirl production. This fact was acknowledged by Chigier and Beer,[2] Pratte and Keffer,[3] and others. The design of swirl generators in practice today use the following principles of swirl production: 1) adjustable vanes, 2) tangential blowing on the wall of a pipe with axial through flow, 3) spinning, fully-developed pipe flow emerging from a long rotating tube (~ 100 diameters long) and 4) flow through a rotating perforated plate, among others. References 4 and 5 can be consulted on the details of various swirl generator designs and their corresponding limitations and efficiencies.

A number of theoretical studies covering laminar, turbulent, weak and strong swirling jets have been carried out in the past. Görtler[6] performed analytical studies of an incompressible laminar jet in the limit of very weak swirl. In this limit, the radial pressure gradient may be ignored, i.e. p = p(x) only; moreover, a linearization of the momentum equations in swirl velocity is admissible. Based on these and the boundary-layer approximation of the Navier-Stokes equations, Görtler reduces the evolution of a weakly swirling laminar jet problem to an eigenvalue problem of an ordinary, second-order differential equation. Furthermore, upon finding a suitable

2

transformation for the dependent and independent variables, the governing differential equation is transformed into a Legendre type, for which exact solutions are derived. By replacing the kinematic viscosity with an effective constant-eddy viscosity, Görtler generalizes his theory to include turbulent, weakly swirling free jets as well. A theory is proposed by Steiger and Bloom[7] in which incompressible and compressible, axially symmetric laminar free mixing (e.g. wakes and jets) with small, moderate, and large swirl can be examined. The tangential and axial velocity components and the stagnation enthalpy are assumed to have polynomial profiles in the radial direction. The assumption of very small radial velocity allowed the use of boundary-layer-type formulations in the analysis. The von Kármán integral method then is applied to the viscous layer (i.e., the wake) of a rotating axisymmetric body with no comparison to experimental data. Lee[8] has obtained closed-form solutions for an axisymmetric turbulent swirling jet using similarity assumptions for the axial and the tangential velocities. The radial and axial velocities are linked via an entrainment assumption, after Taylor.[9] The theoretical predictions are compared to the experimental data of Rose,[10] where close agreement in the case of weak swirl is demonstrated. The experimental data reported by Rose[10] were collected in a swirling turbulent jet issuing from a long rotating tube. Lee's assumptions of the Gaussian axial velocity distribution and the corresponding similar tangential velocity profile were directly deduced from Rose's experiment, where similarity conditions were observed for $x/D > 1.5$.

Chigier and Chervinsky[11,12] have performed theoretical and experimental studies of turbulent swirling jets issuing from a round orifice. They used boundary-layer approximations for assumptions of similar profiles to integrate the equations of motion for incompressible turbulent flows. The similarity

assumption was experimentally demonstrated to hold in a swirling jet for weak and moderate swirls, for x/D > 4. For strongly swirling flows, where the mean axial velocity distribution shows a central trough, or what is also known as a double-hump profile, the similarity was not observed until 10 diam. For x/D > 10, the location of the maximum mean axial velocity shifted back to the jet centerline, from which point the similarity was observed. The measured mean axial velocity and static pressure profiles were described by Gaussian error curves, and the mean tangential velocity profile was expressed in terms of third-order polynomials. The empirical constants in the data-fit expressions of Chigier and Chervinsky are functions of the degree of swirl in the jet defined as

$$G \equiv W_{mo}/U_{mo} \qquad (4)$$

the ratio of maximum mean tangential-to-axial velocity at the nozzle exit.

Mattingly and Oates[13] performed an experimental investigation of the mean, incompressible mixing process in confined coannular swirling flows. In this investigation, the swirl was present in the inner stream only, thereby leading to flow conditions unstable in the sense of Rayleigh (i.e., instability ensuing from an outwardly decreasing angular momentum). Enhanced radial mixing was attributed to the Rayleigh instability.

The latest reviews in the field of confined swirling flows,[14,15] primarily with combustion, reveal an extensive reference list and activities in this area of research. For a more comprehensive and recent work on the predictions and measurements of the swirling flows in combustor geometries, Ref. 16 may be consulted.

Kerrebrock[17] has proposed a general theory for the small-disturbance field in strongly swirling flows in turbomachine annuli. He concluded that small amplitude "shear" disturbances are not purely convected but rather

4

propagate slowly in flows stable in the sense of Rayleigh and are unstable in flows approaching free vortex.

Extensive literature exists on the phenomenon of vortex breakdown or flow reversal and vortex instability in strongly swirling flows. References 18-20 are among the most fundamental. Despite significant strides, a comprehensive theoretical description of the phenomena leading to vortex breakdown still does not exist. The various theoretical ideas of hydrodynamic stability and finite transition to a subsequent state (analogous to hydraulic jump) that are proposed provide only partial insight into this complex flow phenomenon. For an exhaustive list of references and critical evaluation of the proposed theories, Refs. 21-23 should be consulted. The special problem of the bursting of leading-edge vortices (e.g., over delta wings) is examined in Refs. 24-25. In a recent contribution Shi et al.[26] have experimentally investigated the location and control of vortex breakdown over a delta wing of high sweep angle.

Common to all the previous methods of swirl generation in free jets and ducts, as described in the experimental swirl research articles, is the production of near-solid-body rotation flows. An exception to this is found in a recent contribution by Samimy et al.,[27] who generated forced and free-vortex swirl distributions in their facility. Details of swirl generator design employed by Samimy et al. is described in Ref. 28.

Controlled excitation of nonswirling jets has been extensively studied in the past few years by many investigators including Crow and Champagne,[29] Chan,[30,31] Moore,[32] Hussain and Zaman,[33,34] and Ahuja et al.[35] Excitation at the right level and Strouhal number has been shown to result in a faster spread rate due to the higher entrainment caused by the engulfing

action of the large-scale coherent structures in the initial region of the mixing layer.

Zaman and Hussain[36,37] showed that turbulence in a circular nonswirling jet is enhanced by excitation at Strouhal numbers between 0.2 and 0.8 and is suppressed between 2 and 4. They also concluded that enhancement or suppression of turbulence not only depends on the excitation Strouhal number but also is affected by the nature of the nozzle boundary layer (i.e., laminar, transitional, or turbulent). Moore[32] and Ahuja et al.[35] showed that the threshold level of the acoustic pressure excitation for effective turbulent mixing, and a consequential jet noise amplification, can be taken to be 0.08 percent of the jet dynamic pressure at the correct Strouhal number.

As noted earlier, swirling flows are primarily driven in the near field $(x/D < 5)$ by the static pressure gradients in both axial and radial directions. Swirling jets are also inherently highly turbulent. The above characteristics make these flows not easily responsive to any kind of excitation. Mixing enhancement and control of swirling flows are of interest, however, from the point of view of improving the performance of many engine components such as combustion chambers and rotating turbomachinery, as well as vortex-lift devices for external aerodynamics.

The recent study of the controlled excitation of a cold turbulent swirling jet by the authors[5,38,39] was the first experimental attempt towards basic understanding of this phenomenon. The experiments were conducted for a flow with swirl number of 0.35 (defined as the ratio of the flux of angular momentum to axial momentum normalized by nozzle exit radius). The time-mean axial velocity distribution did not have a "top-hat" radial profile at the nozzle exit. The excitation level of plane acoustic waves was held constant at 124 dB at various Strouhal numbers. The results

6

showed that even though the axial velocity distribution at the nozzle exit did not have a "top-hat" profile, the instability waves were amplified rapidly in the streamwise direction, reaching a maximum in amplitude and then decaying further downstream. Excitation at a Strouhal number of 0.4 exhibited the largest growth. Furthermore, it was observed from these results that the instability waves peaked closer to the nozzle exit and their maximum amplitudes were only about 50 percent of their counterparts in the nonswirling jet having the same mass flux, Mach number, and Reynolds number.

The authors in Ref. 40 further investigated the excitability of swirling jets by plane acoustic waves. The emphasis of the research was to study the influence of excitation on mean flow characteristics. To accomplish this, a new acoustic driver system capable of providing much larger excitation amplitudes was used. also the experiments were conducted at lower swirl numbers than the previous experiments and with radial profiles of axial velocity that were more nearly "top hat." Effects of swirl number on jet excitability were studied by comparing the response of two jets at different swirl numbers to acoustic excitation. Some comparisons of the results with those of a nonswirling jet generated in the same facility are also made.

Qualitative behavior of a swirling turbulent jet in response to single-frequency, plane acoustic excitation was visualized by Farokhi, Taghavi, and Raman[41] via Schlieren optics. Periodic vortex sheet roll-up in the form of large-scale coherent structures was promoted in the swirling turbulent shear layer via plane acoustic excitation. These structures were evidenced on many photographs. Furthermore, the emergence of nearly axisymmetric vortex rings in the shear layer of a swirling jet excited by plane acoustic waves was noteworthy.[41]

Some of the more significant results of passive and active control of turbulent shear layer with swirl investigated at NASA-Lewis Research Center are presented in this paper after a brief description of the experimental facility.

2. Experimental Facility

2.1 Swirl Generator

Figure 1 is a schematic diagram of the test setup. An existing cold-jet facility at NASA Lewis Research Center was modified to generate flows at a wide range of swirl numbers. The principle of combining axial and tangential streams is applied for swirl generation. Axial air is introduced through a 20.32 cm (8 in.) pipe at the end of the plenum. Tangential air enters the plenum chamber through 54 elbow nozzles mounted on three concentric circular rings as shown in Figs. 1 and 2. Specially designed restrictors and screens are inserted into the elbow nozzles to reduce the orifice noise generation. The nozzle exit plane is of a multihole design that also contributes to the nozzle's low-noise character. Swirl number can be adjusted by remote control valves which vary the proportion of axial to tangential air. The flow leaving the swirl generator passes through a bellmouth and an excitation section before discharging to the test cell through an 11.43 cm (4.50 in.) diameter nozzle. For more details regarding the swirl generator and test facility see Ref. 5.

2.2 Instrumentation

Three components of time-mean velocity, as well as static and total pressures, were measured by a five-hole pitot probe having a diameter of 0.125 in. (0.318 cm) at the measuring tip. The probe tip has a 45° cone angle, and the pressure ports are located at the midspan of the conical surface. The five-hole probe is self nulling in the yaw direction, while the pitch angle, time-mean velocity components, and mean pressures are computed from the measured pressures and the probe calibration curves. For further details, Refs. 5 and 38 may be consulted.

9

The axial component of fluctuating velocity was measured along the jet centerline using a TSI model 1260A-10 hot-wire probe and a DISA model 55M01 constant temperature anemometer employing a DISA model 55M25 linearizer. Along the jet axis, the tangential and radial velocity components are negligible compared to the axial component; and therefore the results from a single-element hot-wire probe were assumed to represent the actual streamwise velocity fluctuations. The fundamental-rms amplitude at each streamwise location was obtained by analyzing the hot-wire spectra at the excitation frequency. Even though no phase-averaging technique was applied, the amplitude of the fundamental wave was significantly above the background noise, which insured negligible contamination of the instability wave amplitude with background turbulence noise. To prevent the probe holder support from entering the flow field and contaminating the data due to its vibration, only half traverses were made starting from the jet centerline for both hot-wire- and five-hole-probe measurements.

Excitation sound pressure level and fluctuating pressure spectra, at the center of the nozzle exit, were measured using a model 4135 (B & K) microphone. The microphone has an outside diameter of 0.25 in. (0.64 cm) and was fitted with a bullet-head fairing. The sound-pressure level in dB (re. 20 μPa) at the excitation frequency was obtained from the spectra of the microphone signal using a Wavetek model 804A signal analyzer.

3. Results and Discussion

3.1 Passive Control

The experimental results presented in this section are time-averaged data gathered from two swirling jets generated separately by the manifolds A and C. The swirl number in both jets was held constant at 0.48 and the mass-averaged, mean axial Mach number at the nozzle exit was ≈ 0.14. The Reynolds number based on the mean axial velocity and the nozzle diameter was 375,000 in both cases. Figure 3 is a definition sketch showing the coordinates and the mean velocity components in the jet.

The two extreme tangential velocity distributions investigated in our facility are plotted in Fig. 4. The vortex core size generated by the manifold C, at $x/D = 0.06$, is about one quarter of the nozzle exit diameter, whereas that of the manifold A spans across the full exit plane.

Widely different axial evolution of the mean axial velocity profiles for the two swirling jets generated by the manifolds A and C is noted from Figs. 5a and 5b, respectively. The large-core vortex flow, (Fig. 5a), shows a continuous gradual decay of the mean axial velocity component along the jet. The small core-vortex flow, (Fig. 5b) demonstrates a central trough or a double-hump profile associated with the swirl numbers higher than 0.48 (namely 0.6). The mean centerline velocity on the jet axis, i.e. $r/D = 0$, in Fig. 5b shows a rapid initial deceleration followed by an acceleration period that has never been reported, to our knowledge, for S = 0.48 jets. Upon further examination of the mean axial velocity between three and four nozzle diameters, we observed that the small-core-vortex jet with S = 0.48 was on the verge of vortex breakdown, as shown in Fig. 6. The forward and rear stagnation points, both very close to the jet axis, exhibited an unsteady behavior, as had been noted in the earlier vortex breakdown experiments. The

11

fact that a swirling jet has been brought to the point of breakdown at a swirl
number (i.e., 0.48) significantly lower than the critical value was assumed to
be (i.e., $S_{crit} \gtrsim 0.6$) is the most remarkable result of our mean-flow
investigation. Examining Fig. 5b for the condition of axisymmetry reveals
that the mean axial velocity distribution associated with the small-core
vortex does not achieve near axisymmetric behavior until four nozzle
diameters. This is in contrast to the mean tangential velocity profile, which
exhibited axisymmetric property in one nozzle diameter.

Finally, the decay of the mean axial velocity along the jet axis is
presented in Fig. 7. The swirling jet produced by manifold C is on the verge
of breakdown, while that of manifold A exhibits classical behavior for this
level of swirl number, i.e., 0.48. The instantaneous behavior of the
incipient vortex breakdown is depicted in Fig. 7 by broken lines. Due to
highly unsteady nature of the stagnation point associated with a (bubble-type)
vortex breakdown, the time-averaged measurements on the jet axis do not fully
resolve this behavior.

3.2 Active Control

In a flow visualization study, Farokhi, Taghavi, and Raman[41]
investigated the response of a warm swirling jet to a single-frequency, plane-
acoustic wave excitation via Schlieren optics. The promotion of periodic
large-scale coherent structures in the near field of a turbulent swirling jet
is evidenced in Fig. 8. This qualitative investigation demonstrated the
excitability of a turbulent shear layer with swirl, even to plane wave forcing
at "preferred" frequencies. The first quantitative attempt to study the
growth characteristics of the fundamental disturbance wave along the axis of a
swirling turbulent jet was performed by the authors.[39]

To examine the effect of excitation on the swirling jet, and compare with the excited nonswirling jet, both flows were excited internally by plane acoustic waves upstream of the nozzle inlet. To isolate the effect of excitation frequency, the sound pressure level was kept constant at 126 dB for both jets at all excitation frequencies, measured at the center of the nozzle exit.

Figures 9 and 10 illustrate the growth of the instability waves triggered at different excitation frequencies for the nonswirling and swirling jets, respectively. It was observed that the swirling jet under investigation as well as the nonswirling jet were excitable by plane acoustic waves. At equal excitation frequencies, the instability waves grew about 50 percent less in peak r.m.s. amplitude in the swirling jet as compared to the nonswirling jet. This difference is not unexpected, as linear instability theory states that the stability of the free shear layers depends upon the detailed velocity distributions. Here we are dealing with two jets which are entirely different as far as velocity and pressure distributions are concerned. It is also expected that the growth of the instability waves should also depend upon the swirl number which affects the velocity and pressure distributions.

For the nonswirling jet, the location of the maximum growth of the instability waves was approximately at the end of the potential core (x = 4.0D). This is in agreement with the observation in the literature that the axisymmetric disturbances achieve their peak amplitude near the end of the potential core.[42] For the swirling jet, the potential core does not exist and the maximum growth occurs at about x = 2.5D. This location should also depend on swirl number.

The variation of the peak r.m.s. amplitude of the axial velocity fluctuations on the jet axis versus the Strouhal number ($St = f \cdot D/U_a$) is

13

plotted in Fig. 11. From this figure it is observed that the maximum growth of the instability wave is measured at a Strouhal number of 0.4, based on mass-averaged axial velocity at the nozzle exit for both cases. This is in agreement with the results quoted in the literature for the nonswirling axisymmetric jets.[32]

Even though significant improvement in jet mixing, as a result of excitation, was measured in our facility for nonswirling jets,[43] no change was observed in the mean velocity components of the swirling jet due to excitation. Two plausible explanations may be forwarded: (1) the presence of strong static pressure gradients in the near field of a swirling jet (with moderate to strong swirl) overwhelms the turbulence-induced shear layer growth, and (2) higher initial turbulence level of the swirling jet as compared to its nonswirling counterpart dampens the growth of the shear-layer instability wave. The effect of core turbulence intensity on the mixing and excitability of an axisymmetric, nonswirling cold free jet is examined by Raman et al.,[44] which supports our argument.

To investigate the effect of larger-amplitude acoustic excitation on the evolution of a swirling turbulent jet, the cold jet facility at NASA-Lewis Research Center was modified, as shown in Fig. 12. Plane acoustic waves were generated by two Lind Model EPT-94B electro-pneumatic acoustic drivers, positioned 180° apart around a 16.14 in. (41 cm) cylindrical section and operated in phase. Each driver is an electrically-controlled air modulator capable of generating 170 dB SPL in the near field. The drivers were operated by an air supply of 124 psig (87 184 kg/m^2) at a maximum flow rate of 0.6 lb/sec (0.27 kg/sec). The air leaving the drivers wad directed in the tangential direction by means of scoops just inside the plenum. After leaving the plenum, the swirling air was passed through a 30 mesh screen and a trip-

ring before entering the 3.5 in. (8.89 cm) diameter nozzle. The screen and trip-ring were located 13 in. (33 cm) upstream of the nozzle exit where the diameter of the contracting section was 5.16 in. (13.1 cm). The nozzle had an 8.66 in. (22 cm) long cylindrical section prior to its exit.

In this study, the excitability of a swirling jet, with a mass-flow rate of 1.2 lb/sec (0.54 kg/sec) was experimentally investigated. The experiments were conducted by exciting a free jet with a swirl number of S = 0.12 by plane acoustics waves. The maximum time-mean tangential and axial velocities at the nozzle exit plane were 58.8 fps (17.9 m/sec) and 275 fps (83.8 m/sec), respectively. The respective Mach and Reynolds numbers of the jet based on the mass-averaged axial velocity at the nozzle exit were 0.22 and 460 000. The maximum forcing amplitude of the excitation was 6.88 percent of time-mean axial velocity at a Strouhal number of St = 0.39, measured at the center of the nozzle exit plane. The variation of the rms amplitude of velocity fluctuations at the fundamental excitation frequency(u_f') along the jet centerline, corresponding to various excitation Stouhal numbers, is shown in Fig. 13. The "preferred" Strouhal number based on the nozzle exit diameter, mass-averaged axial velocity, and excitation frequency was about 0.39 as indicated in the figure. The forcing amplitude of the excitation at this frequency was 6.88 percent of the time-mean centerline axial velocity at the nozzle exit (u_{fe}'/U_{ce}). The axial location of the "saturation" point was at x/D = 2. The growth and decay of the instability wave agrees with the data of Raman et al.[44,45] for highly turbulent nonswirling jets excited at high amplitudes.

Figure 14 shows the streamwise evolution of velocity spectra along the jet axis at an excitation frequency of 330 Hz (St = 0.39). The isolated peaks at 660 Hz (first harmonic) and 990 Hz (second harmonic) were not amplified by

the flow and therefore not considered in this study. Also from this figure, it is clear that no growth of the subharmonic (165 Hz) is experienced in the case of the swirling jet excited by plane waves. This observation is quite different from that of the nonswirling jets, in which considerable growth of the subharmonic is measurable as a result of excitation at St. = 0.5.[16]

Distributions of total axial turbulence intensity along the jet centerline for the unexcited and excited (St = 0.39) cases are compared in Fig. 15a. It is seen that as a result of excitation, the total axial turbulence intensity at the nozzle exit has been almost doubled and the location of its maximum value on the jet axis has moved upstream from x/D = 6 to x/D = 2.5. For a similar excited jet without swirl, the peak value is reached at a location much further downstream (x/D = 9).[44]

As the main purpose of exciting the jet is usually to enhance mixing, alterations in mixing can be observed by comparing the mean flow parameters with and without excitation. The decay of the time-mean axial velocity along the jet axis is compared for excited and unexcited cases in Fig. 15b. From this figure it is clear that excitation results in a faster decay starting immediately downstream from the nozzle exit. The faster decay of the mean centerline axial velocity is an indication of more jet spreading and enhanced mixing. The enhanced mixing is further confirmed in Fig. 16, where the radial distributions of mean axial velocity at x/d = 7 for excited and unexcited cases are compared. The half velocity radius has increased by about 13.2 percent as a result of excitation.

The variation of momentum thickness along the jet axis for the unexcited swirling jet with swirl number of S = 0.12 is plotted in Fig. 17. The value for the excited swirling jet at x/D = 7 which is also shown indicates an

increase of about 5.8 percent over the unexcited case and is a further indication of enhanced mixing. The momentum thickness used here is defined as

$$\theta = \int_{o}^{\infty} [(U/U_c) \cdot (1 - U/U_c)dr \qquad (5)$$

Data for a similar jet but without swirl[47] are also plotted in the same figure. For a given axial location, this figure indicates that the momentum thickness for the swirling jet is higher than that of the nonswirling jet. This is an indication of higher spread rate of the swirling jet compared to the nonswirling jet at all axial locations. It also indicates that the radial gradient of the time-mean axial velocity for the swirling jet is less than the corresponding value of the nonswirling jet. Since based on the linear stability theory[48] the growth of the instability wave is proportional to the magnitude of the mean axial velocity gradient, then at a given location along the jet centerline, the instability wave has a lower growth rate for the swirling jet as compared to the nonswirling jet under the same conditions. Therefore, the effect of excitation on a swirling jet is less pronounced compared to the nonswirling jet. This also suggests that mixing enhancement of swirling jets by excitation requires forcing at higher amplitudes compared to the nonswirling jets.

To investigate the effect of swirl number on jet excitability, the 30-mesh screen, which was located upstream of the nozzle, was removed. As a result, the maximum time-mean axial and tangential velocities were increased to 286 fps (87.2 m/sec) and 86.3 fps (26.3 m/sec), respectively, as shown in Figs. 18a and 18b. The swirl number was consequently increased from S = 0.12 to S = 0.18. Distributions of time-mean axial velocity and turbulence intensity along the jet axis for the jets with the two different swirl numbers studied are plotted in Figs. 19 and 20. It seems, from Fig. 19, that with an

17

increase in swirl number and with no excitation, the decay of time-mean axial velocity started further upstream and almost immediately after the nozzle exit, and the "nominal" potential core disappeared. The turbulence intensity at the nozzle exit is also increased for the higher swirl number case by about 60 percent, and the downstream location of its maximum value is moved further upstream from x/D = 6 to about x/D = 3 (Fig. 20).

The jet, with the higher swirl number of S = 0.18, was then excited at the same amplitude as before and at various frequencies. Even though the instability waves exhibited growth along the jet axis (data not shown in this paper), no effect on spread rate and mixing enhancement was observed as a result of excitation. In addition to the issue of decreased radial gradient of axial velocity which was discussed before, another possible explanation for the above can be seen from Fig. 20. The distribution of turbulence intensity along the jet axis for the unexcited jet at the higher swirl number of S = 0.18 almost coincides with that of the excited jet with S = 0.12. Therefore, the higher swirling jet seems to be self excited and consequently may be insensitive to any additional excitation. The higher initial turbulence of the jet with swirl number of S = 0.18 compared to the jet at S = 0.12 might also be another explanation for unexcitability of this jet.[46] According to this reference, "increasing the upstream turbulence diminishes the excitability of the jet and reduces the effect of excitation on the spreading rate of the jet.

According to hydrodynamic stability analysis of swirling flows[49-51], nonaxisymmetric disturbances, i.e., infinitesimal helical waves spinning in the opposite direction to the rotating flow tend to grow faster than the plane wave disturbances in the near field. Consequently, the excitation section of the free shear-layer control facility at NASA-Lewis Research Center was modi-

fied to provide the above-mentioned capability. Figure 21 shows eight acoustic drivers surrounding the nozzle exit plane capable of high-amplitude nonaxisymmetric forcing of the turbulent shear layer. The helical and axisymmetric excitation of unstable (mean) swirling flows, in the sense of Rayleigh, is also under current investigation in our research facility. Finally, we propose to investigate multifrequency, multimodal internal and external excitation of turbulent shear layers with swirl, including the effect of forcing on vortex breakdown.

4. Concluding Remarks

Free turbulent jets and wakes with swirl experience streamwise and cross-stream pressure gradients unlike the nonswirling free shear-layer flows. Hence, in the near field, the jet (or wake) spread mechanism is pressure-gradient dominated and therefore inviscid. Variation of initial swirl distribution offers the strongest passive control technique for the mean free shear-layer evolution. Turbulent swirling jets are shown to be excitable via single-frequency, plane-wave forcing. Growth and saturation of the fundamental wave in the vortex core exhibit similar qualitative behavior to the nonswirling jets and are found to be swirl-number dependent. Large-amplitude excitation is necessary to overcome the inherently larger turbulence intensities in the rotating shear layers. Enhanced mixing or faster jet spread is achieved in a subsonic swirling turbulent jet by plane-wave acoustic excitation. Guided by hydrodynamic stability analysis of swirling flows, nonaxisymmetric disturbances of negative helicity are targeted as excitation instability waves for control and mixing enhancement of rotating shear layers. New capabilities in multimodel forcing and resonant wave interaction with the preferred modes of a swirling jet offer exciting new opportunities for active flow control research.

References

1. Farokhi, S., Taghavi, R., and Rice, E. J., "Effect of Initial Swirl Distribution on the Evolution of a Turbulent Jet," _AIAA Journal_, Vol. 27, No. 6, June 1989, pp. 700-706.

2. Chigier, N.A., and Beer, J.M., "Velocity and Static Pressure Distributions in Swirling Air Jets Issuing from Annular and Divergent Nozzles," _Transactions of the ASME, Journal of Basic Engineering_, Dec. 1964, pp. 788-796.

3. Pratte, B.D., and Keffer, J.F., "The Swirling Turbulent Jet," Transactions of the ASME, _Journal of Basic Engineering_, Vol. 93, Dec. 1972, pp. 639-748.

4. Gupta, A.K., Lilley, D.G. and Syred, N., _Swirl Flows_, Abacus Press, Tunbridge Wells, England, 1984.

5. Taghavi, R., "Experimental Investigation of Swirling Turbulent Jets," Ph.D. Dissertation, University of Kansas, March 1988.

6. Görtler, H., "Decay of Swirl in an Axially Symmetrical Jet, Far from the Orifice," _Revista, Matemática Hispanoaméricas_, Vol. 14, 1954, pp. 143-178.

7. Steiger, M.H. and Bloom, M.H., "Axially Symmetric Laminar Free Mixing with Large Swirl," _Transactions of the ASME, Journal of Heat Transfer_, Vol. 84-85, Nov. 1962, pp. 370-374.

8. Lee, S.L., "Axisymmetrical Turbulent Swirling Jet," _Transactions of the ASME, Journal of Applied Mechanics_, Vol. 32, June 1965, pp. 258-262.

9. Taylor, G.I., "Dynamics of a Mass of Hot Gas Rising in Air," U.S. Atomic Energy Commission, MDDC-919, LADC-276, 1945.

10. Rose, W.G., "A Swirling Round Turbulent Jet, Part 1: Mean Flow Measurements," _Transactions of the ASME, Journal of Applied Mechanics_, Dec. 1962, pp. 615-625.

11. Chigier, N.A., and Chervinsky, A., "Experimental Investigation of Swirling Vortex Motion in Jets," Transactions of the ASME, Journal of Applied Mechanics, June 1967, pp. 443-445.

12. Chigier, N.A., and Chervinsky, A., "Experimental and Theoretical Study of Turbulent Swirling Jets Issuing from a Round Orifice," Israel Journal of Technology, Vol. 4, No. 1-2, 1966, pp. 44-54.

13. Mattingly, J.D., and Oates, G.C., "An Experimental Investigation of the Mixing of Coannular Swirling Flows," AIAA Journal, Vol. 24, No. 5, May 1986, pp. 785-792.

14. Syred, N., and Beer, J.M., "Combustion in Swirling Flows: A Review," Combustion and Flame, Vol. 23, 1974, pp. 143-201.

15. Lilley, D.G., "Swirl Flows in Combustion: A Review," AIAA Journal, Vol. 15, August 1977, pp. 1063-1078.

16. Rhode, D.L., and Lilley, D.G., "Predictions and Measurements of Isothermal Flowfields in Axisymmetric Combustor Geometries," NASA CR-174916, May 1985.

17. Kerrebrock, J.L., "Small Disturbances in Turbomachine Annuli with Swirl," AIAA Journal, Vol. 15, No. 6, June 1977, pp. 794-803.

18. Benjamin, T.B., "Theory of the Vortex Breakdown Phenomenon," Journal of Fluid Mechanics, Vol. 14, 1962, pp. 593-629.

19. Sarpkaya, T., "On Stationary and Travelling Vortex Breakdown," Journal of Fluid Mechanics, Vol. 45, March 1971, pp. 545-559.

20. Squire, H.B., "Analysis of the Vortex Breakdown Phenomenon," Miszellaneen der Angewandten Mechanik, Berlin, Akademie-Verlag, 1960, pp. 306-312.

21. Hall, M.G., "Vortex Breakdown," Annual Review of Fluid Mechanics, Vol. 4, 1972, pp. 195-218.

22. Leibovich, S., "The Structure of Vortex Breakdown," <u>Annual Review of</u> <u>Fluid Mechanics,</u> Vol. 10, 1978, pp. 221-246.

23. Leibovich, S., "Vortex Stability and Breakdown: Survey and Extension," <u>AIAA Journal,</u> Vol. 22, No. 9, 1984, pp. 1192-1206.

24. Lambourne, N.C., and Bryer, D.W., "The Bursting of Leading Edge Vortices; Some Observations and Discussion of the Phenomenon," Aeronautical Research Council, R & M 3282, 1961.

25. Hall, M.G., "A Theory for the Core of a Leading-Edge Vortex," <u>Journal of</u> <u>Fluid Mechanics,</u> Vol. 11, 1961, pp. 209-228.

26. Shi, Z., Wu, J.M., and Vakili, A.D., "An Investigation of Leading-Edge Vortices on Delta Wings with Jet Blowing," AIAA Paper No. 87-0330, 1987.

27. Samimy, M., Nejad, A.S., Langenfield, C.A., and Favaloro, S.C., "Oscillatory Behavior of Swirling Flows in a Dump Combustor," AIAA Paper 88-0189, Jan. 1988.

28. Buckley, P.L., Craig, R.R., Davis, D.L., and Schwarzkopf, K.G., "The Design and Combustion Performance of Practical Swirlers for Integral Rocket/Ramjet," <u>AIAA Journal,</u> Vol. 21, May 1983, pp. 733-740.

29. Crow, S.C., and Champagne, F.H., "Orderly Structure in Jet Turbulence," <u>Journal of Fluid Mechanics,</u> Vol. 48, Part 3, Aug. 16, 1971, pp. 547-591.

30. Chan, Y.Y., "Spatial Waves in Turbulent Jets," <u>Physics of Fluids,</u> Vol. 17, No. 1, Jan. 1974, pp. 46-53.

31. Chan, Y.Y., "Spatial Waves in Turbulent Jets., Part 2," <u>Physics of</u> <u>Fluids,</u> Vol. 17, No. 9, Sept. 1974, pp. 1667-1670.

32. Moore, C.J., "The Role of Shear-Layer Instability Waves in Jet Exhaust Noise," <u>Journal of Fluid Mechanics,</u> Vol. 80, Part 2, April 25, 1977, pp. 321-367.

33. Hussain, A.K.M.F., and Zaman, K.M.B.Q., "The 'Preferred Mode' of the Axisymmetric Jet," *Journal of Fluid Mechanics,* Vol. 110, Sept. 1981, pp. 39-71.

34. Hussain, A.K.M.F., and Zaman, K.M.B.Q., "Vortex Pairing in a Circular Jet under Controlled Excitation, Part 2: Coherent Structure Dynamics," *Journal of Fluid Mechanics,* Vol. 101, Part 3, Dec. 11, 1980, pp. 493-544.

35. Ahuja, K.K., Lepicovsky, J., Tam, C.K.W., Morris, P.J., and Burrin, R.H., "Tone-Excited Jet: Theory and Experiments," NASA CR-3538, 1982.

36. Zaman, K.M.B.Q., and Hussain, A.K.M.F., "Vortex Pairing in a Circular Jet under Controlled Excitation, Part 1: General Jet Response," *Journal of Fluid Mechanics,* Vol. 101, Part 3, Dec. 11, 1980, pp. 449-491.

37. Zaman, K.M.B.Q., and Hussain, A.K.M.F., "Turbulence Suppression in Free Shear Flows by Controlled Excitation," *Journal of Fluid Mechanics,* Vol. 103, Feb. 1981, pp. 133-160.

38. Taghavi, R., and Farokhi, S., "Turbulent Swirling Jets with Excitation," NASA CR-180895, 1988.

39. Taghavi, R., Rice, E.J., and Farokhi, S., "Controlled Excitation of a Cold Turbulent Swirling Free Jet," *Journal of Vibration, Acoustics, Stress, and Reliability in Design,* Vol. 110, No. 2, Apr. 1988, pp. 234-237.

40. Taghavi, R., Rice, E.J., and Farokhi, S., "Large Amplitude Acoustic Excitation of Swirling Turbulent Jets," AIAA Paper No.89-0970, presented at AIAA 2nd Shear Flow Conference, Tempe, Arizona, March 1989.

41. Farokhi, S., Taghavi, R., Raman, G., "Schlieren Flow Visualization of Axisymmetric Free Jets with Swirl and Excitation," KU-Flight Research Laboratory Report 724-1, October 1987.

42. Petersen, R.A., and Samet, M.M., "On the Preferred Mode of Jet Instability," Journal of Fluid Mechanics, in press.

43. Raman, G., and Ghorashi, B., "Enhanced Mixing of an Axisymmetric Jet by Aerodynamic Excitation," NASA CR-175-59, 1986.

44. Raman, G., Zaman, K.B.M.Q., and Rice, E.J., "Initial Turbulence Effect on Jet Evolution with and without Tonal Excitation," AIAA Paper No. 87-2725, 11th Aeroacoustics Conference, Palo Alto, CA, October 1987.

45. Raman, G., Rice, E.J., and Monkbadi, R., "Saturation and the Limit of Jet Mixing Enhancement by Single Frequency Plane Wave Excitation: Experiment and Theroy," First National Fluid Dynamics Congress, Part 2, AIAA, New York, 1988, pp. 1000-1007 (also NASA TM-100882).

46. Monkbadi, R., Raman, G., and Rice, E.J., "Effects of Core Turbulence on Jet Excitability," AIAA Paper 89-0966, March 1989.

47. Raman, G., and Rice, E. J., "Subharmonic and Fundamental High-Amplitude Excitation of an Axisymmetric Jet." AIAA Paper 89-0993, March 1989.

48. Lin, C.C., The Theory of Hydrodynamic Stability, Cambridge University Press, London, 1955.

49. Howard, L.N., and Gupta, A.S., "On the Hydrodynamic and Hydromagnetic Stability of Swirling Flows," Journal of Fluid Mechanics, Vol. 14, 1962.

50. Lessen, M., Deshpande, N.V., and Hadji-Ohanes, B., "Stability of Potential Vortex with Non-rotating and Rigid Body Rotating Top-Hat Jet Core," Journal of Fluid Mechanics, Vol. 60, 1973.

51. Lessen, M., Singh, P.J., and Paillet, F., "The Stability of Trailing Line Vortex, Part 1: Inviscid Theory," Journal of Fluid Mechanics, Vol. 63, Part 4, 1974.
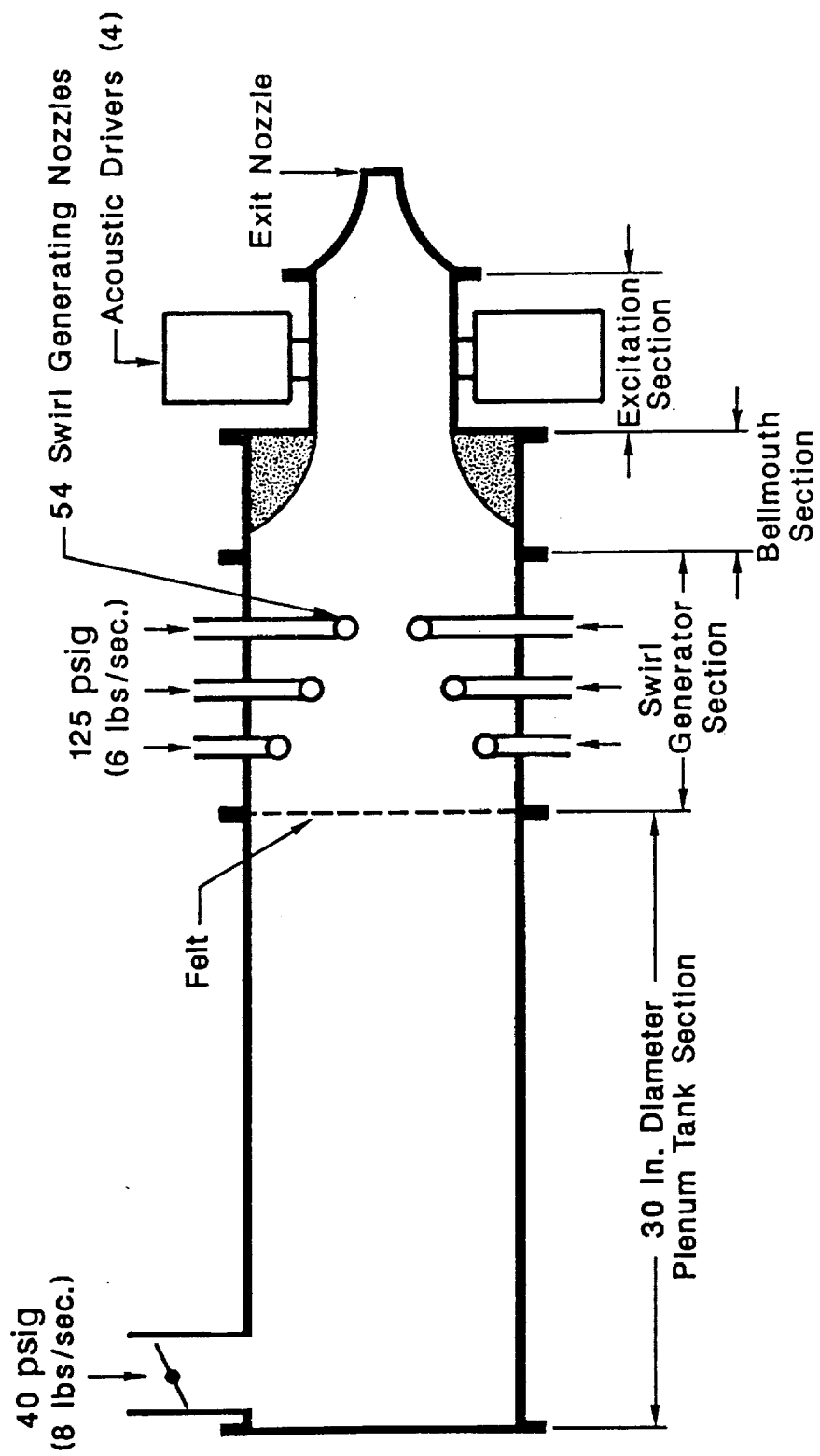
Fig. 1 Schematic diagram of the jet facility.

Manifold A
(24 elbow nozzles)

Manifold B
(18 elbow nozzles)

Manifold C
(12 elbow nozzles)
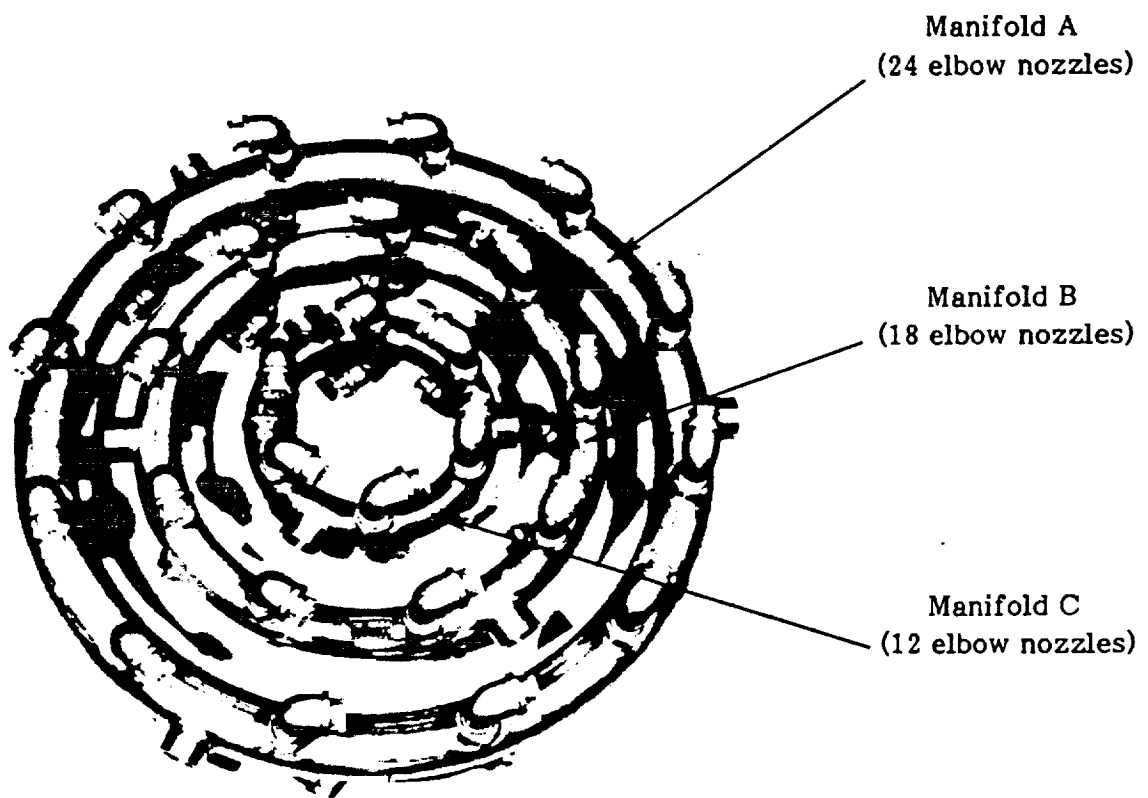
Fig. 2 Manifold rings and elbow nozzles
(unassembled).
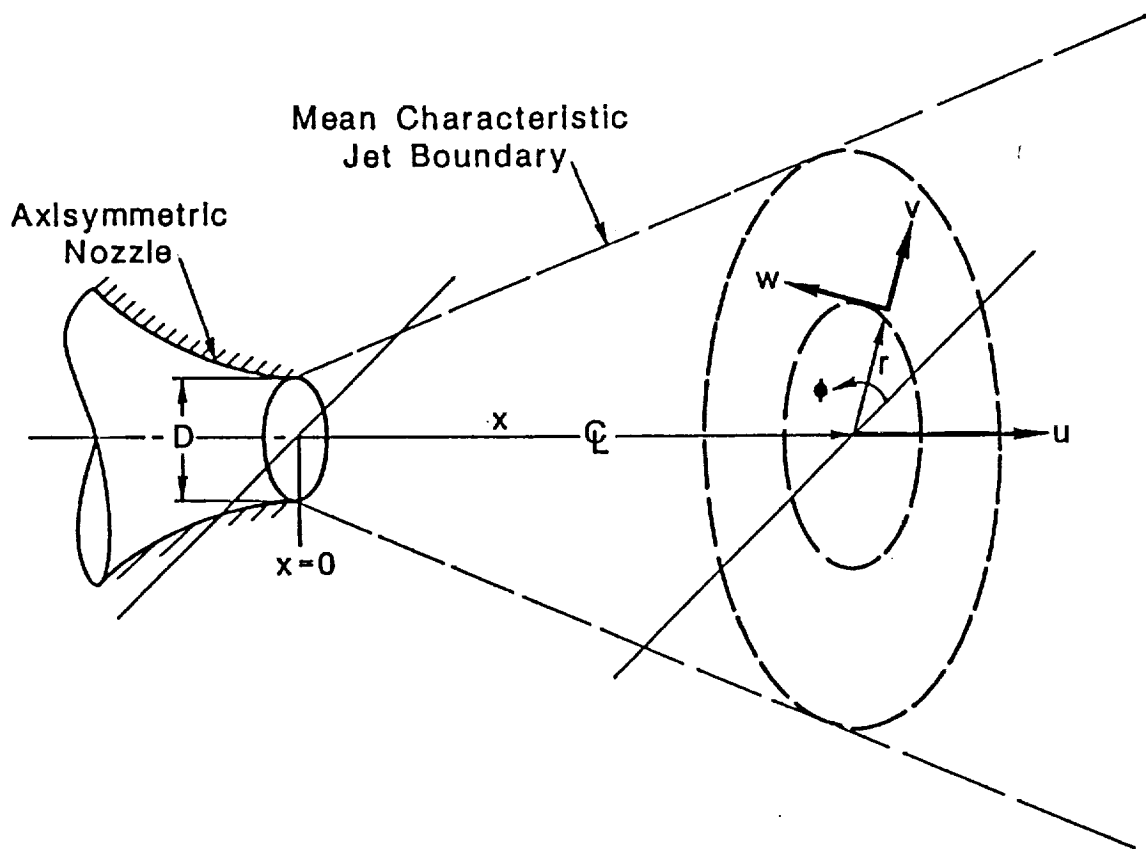
Fig. 3 Definition sketch.
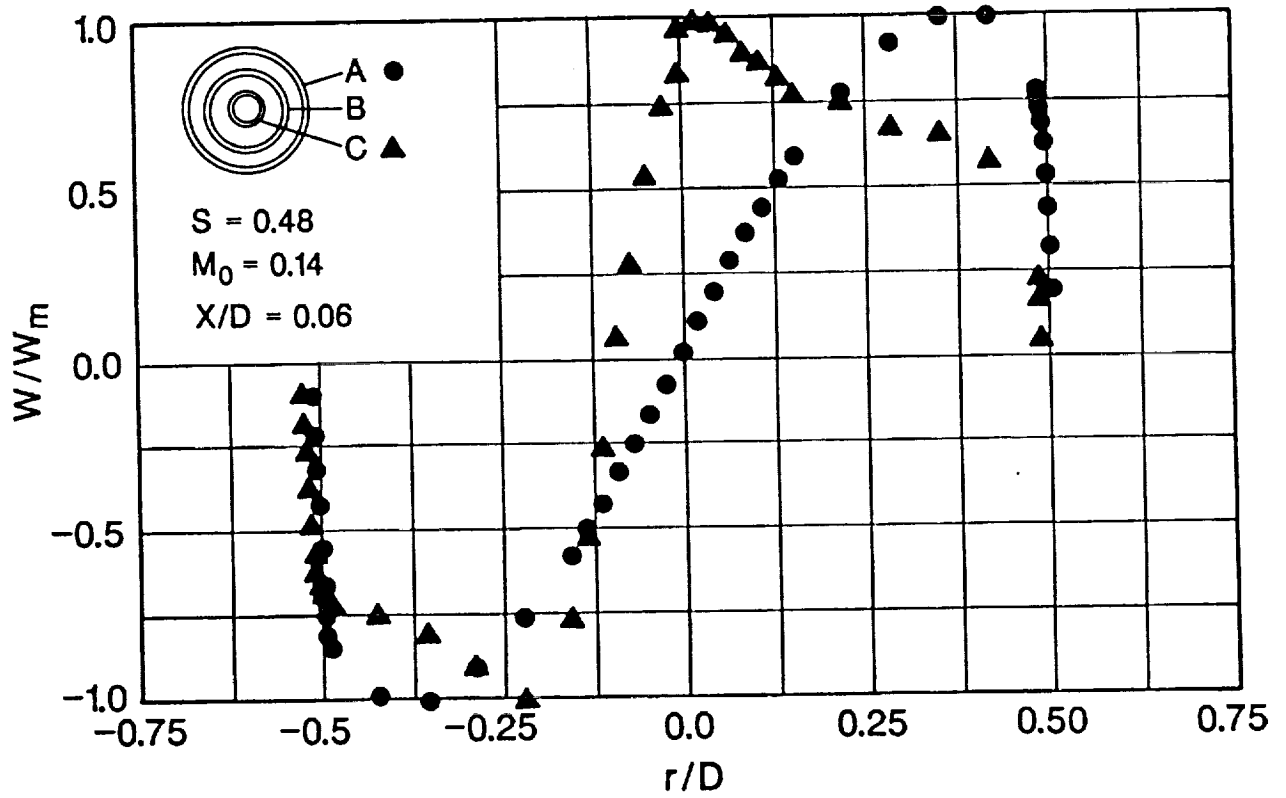
Fig. 4 Radial distribution of the mean
tangential velocity.
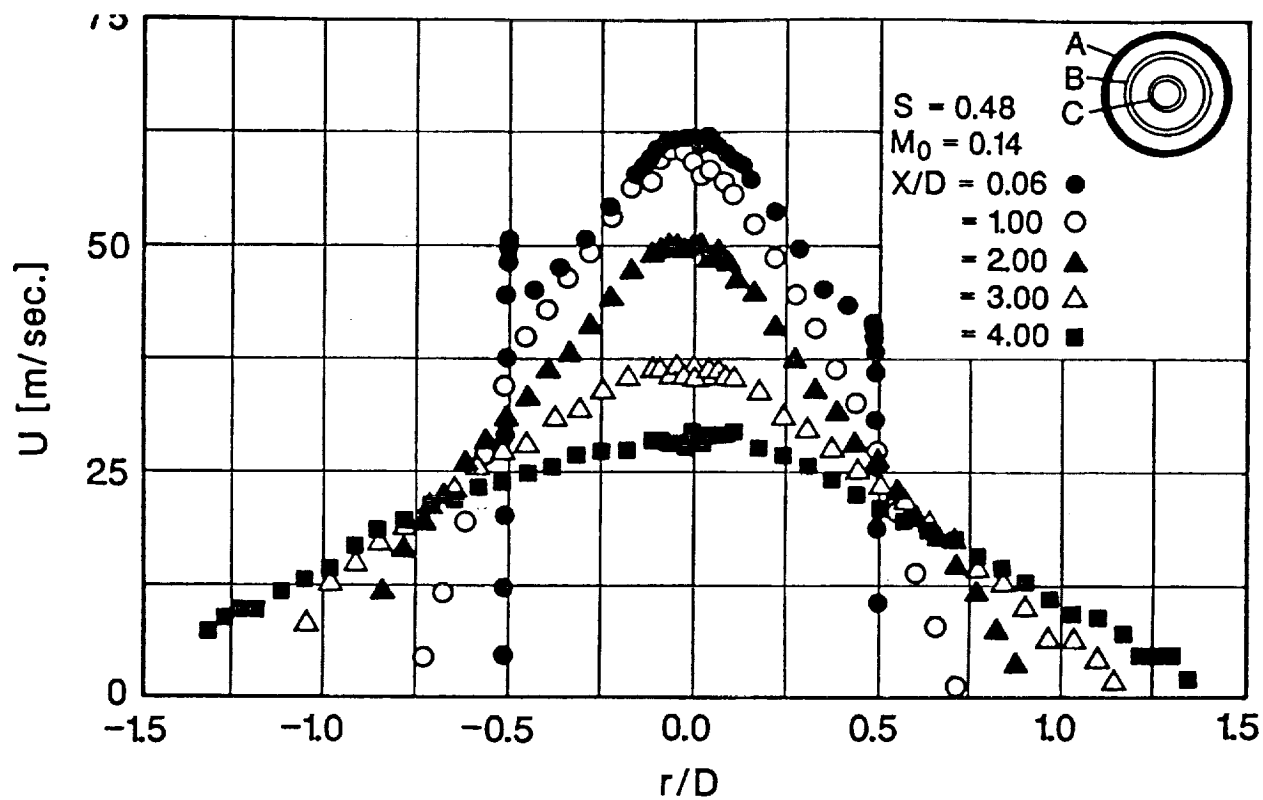
(a) Manifold A
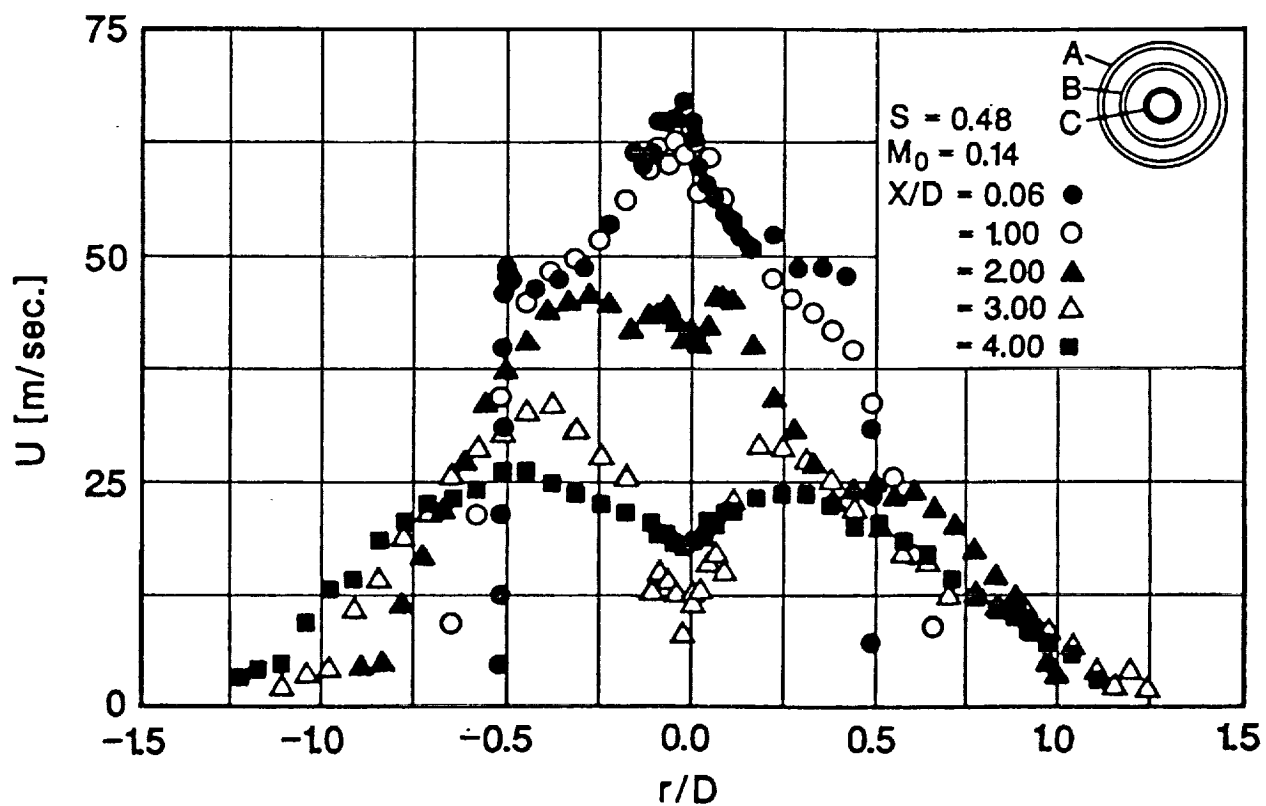
(b) Manifold C

Fig. 5 Downstream development of the mean axial
velocity.
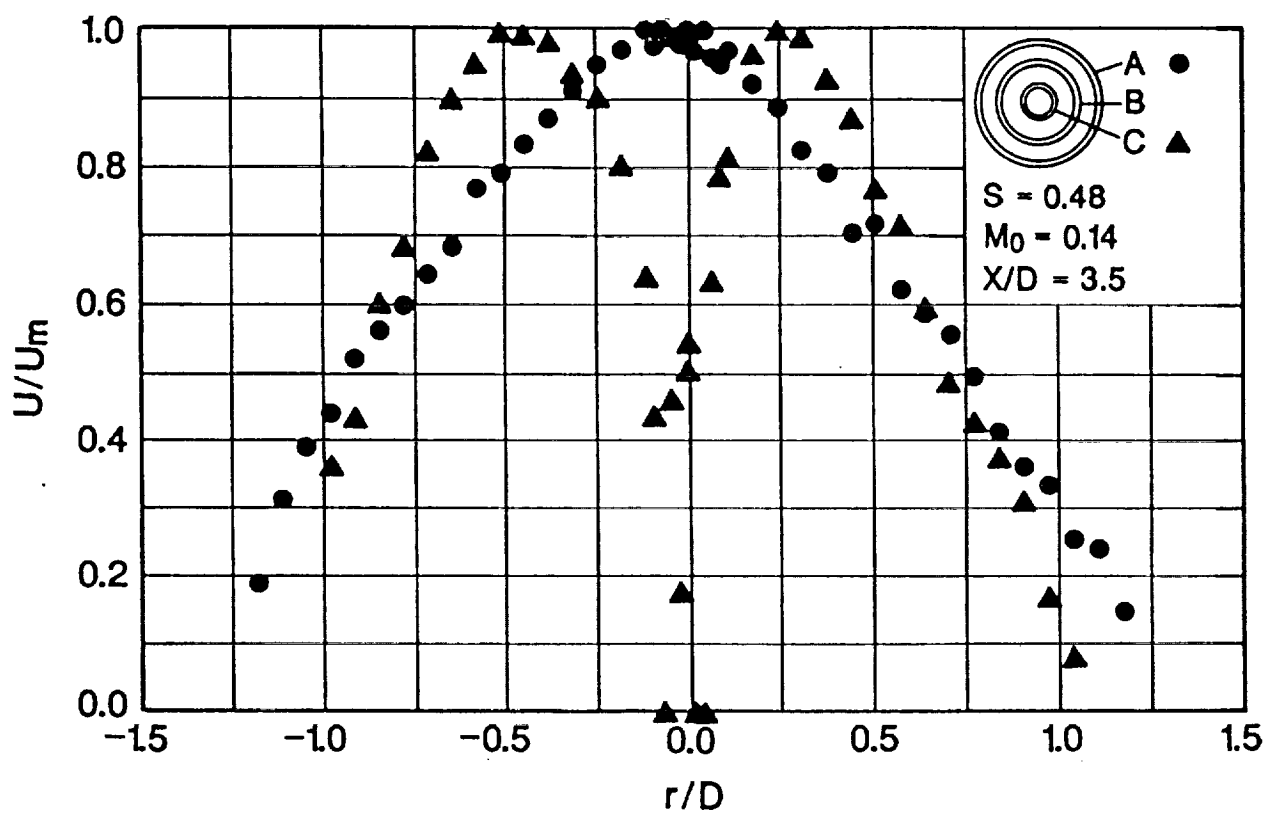
Fig. 6 Radial distribution of the mean axial
velocity.
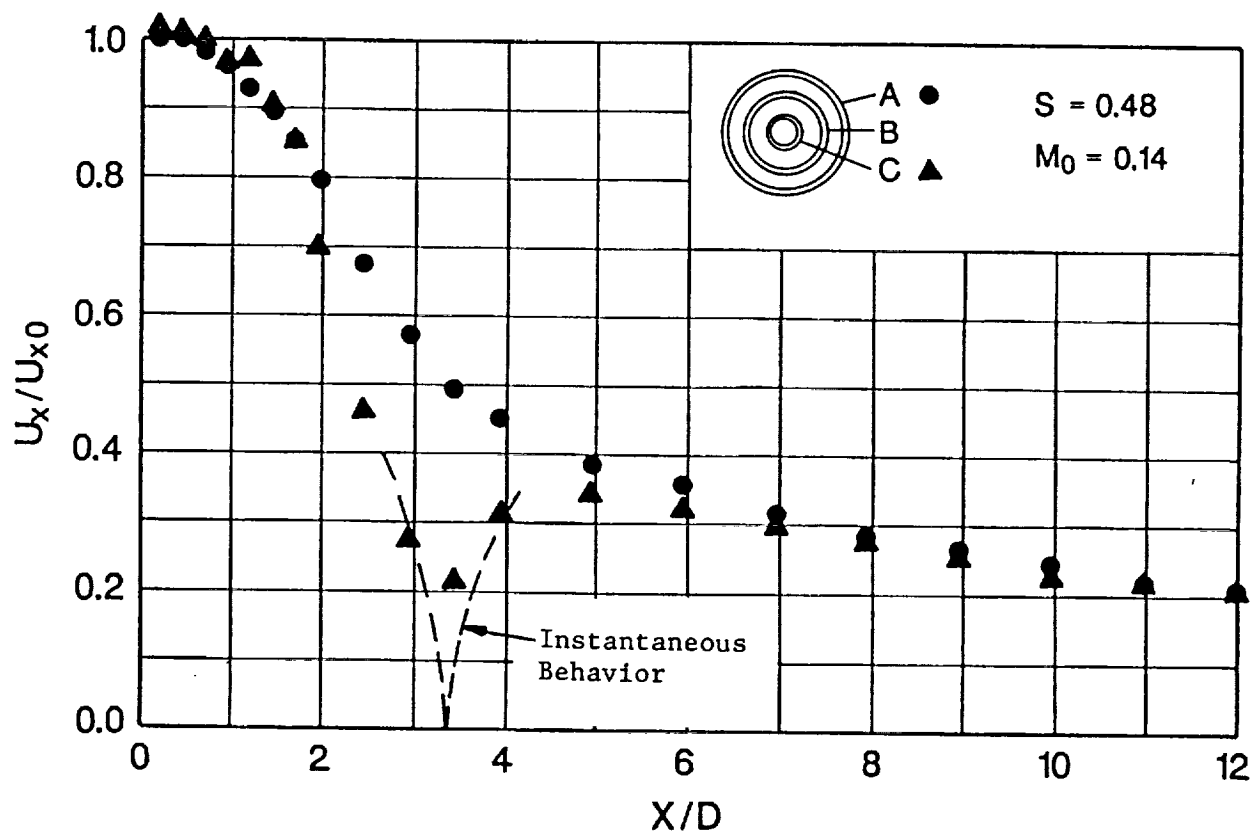
Fig. 7 Decay of the mean axial velocity component
along the jet axis (broken lines depict the
incipient vortex breakdown at x/D = 3.5).
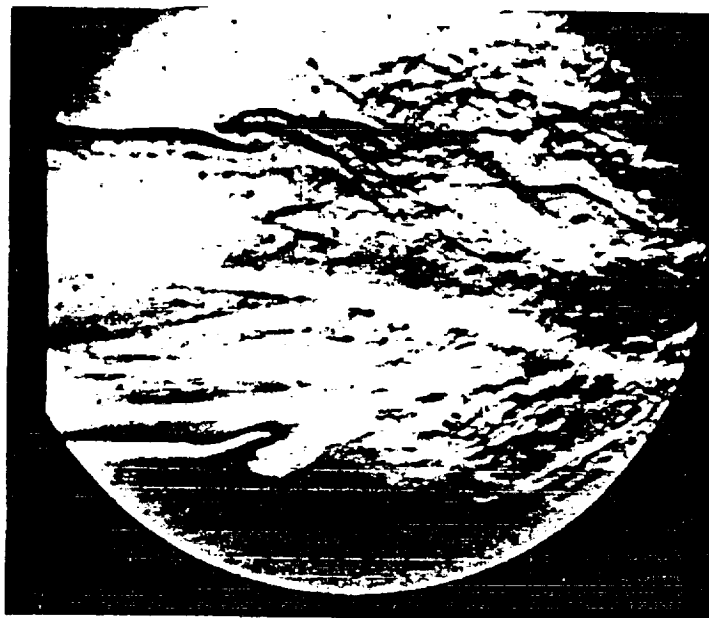
Fig. 8   Schlieren flow visualization of a shear
layer with swirl and excitation.
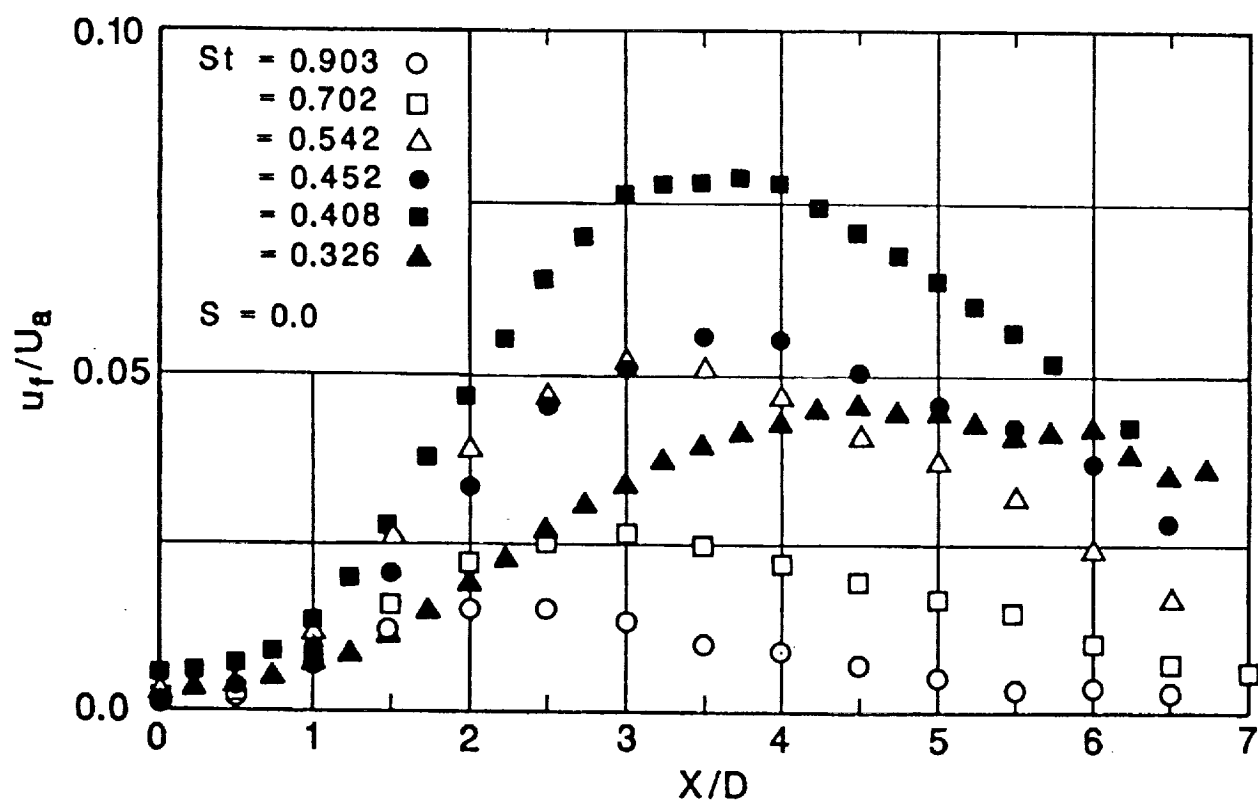
Fig. 9 Variation of fundamental rms amplitude
along the jet axis.
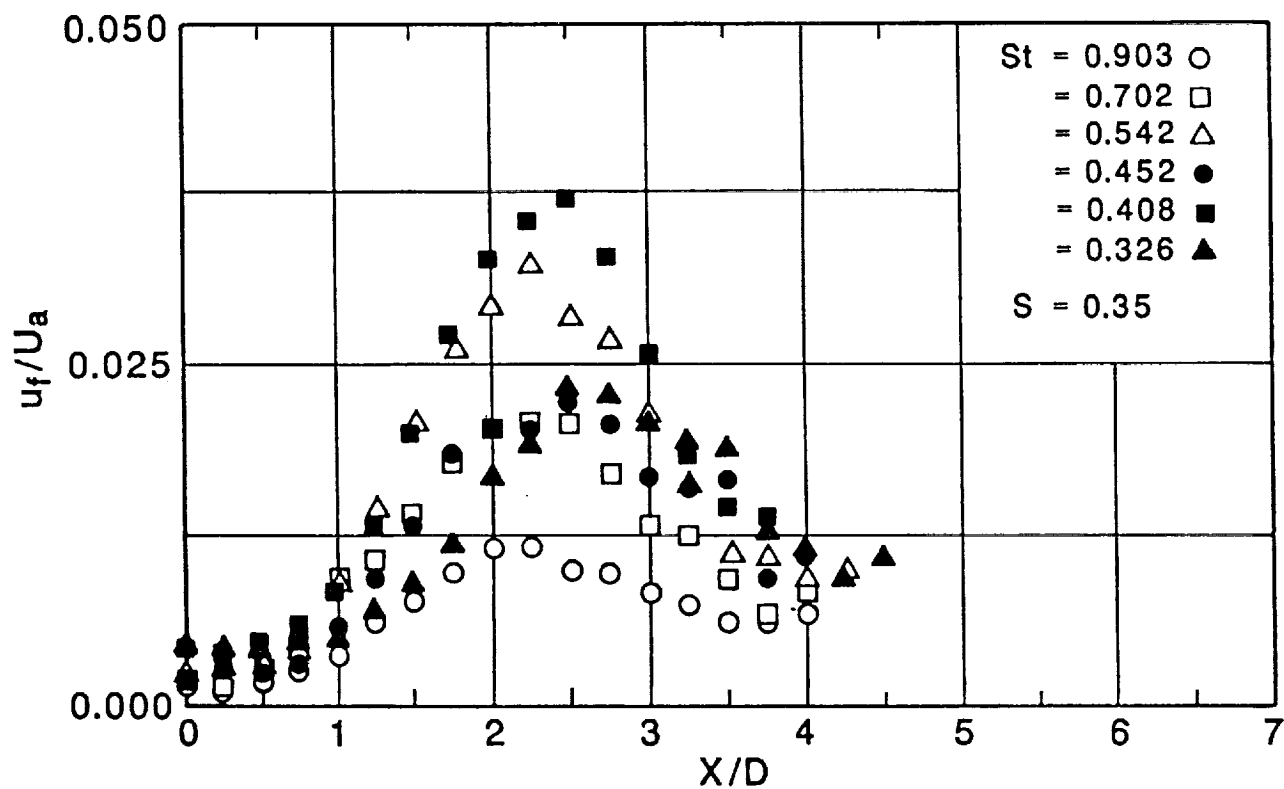
Fig. 10   Variation of fundamental rms amplitude
along the jet axis.
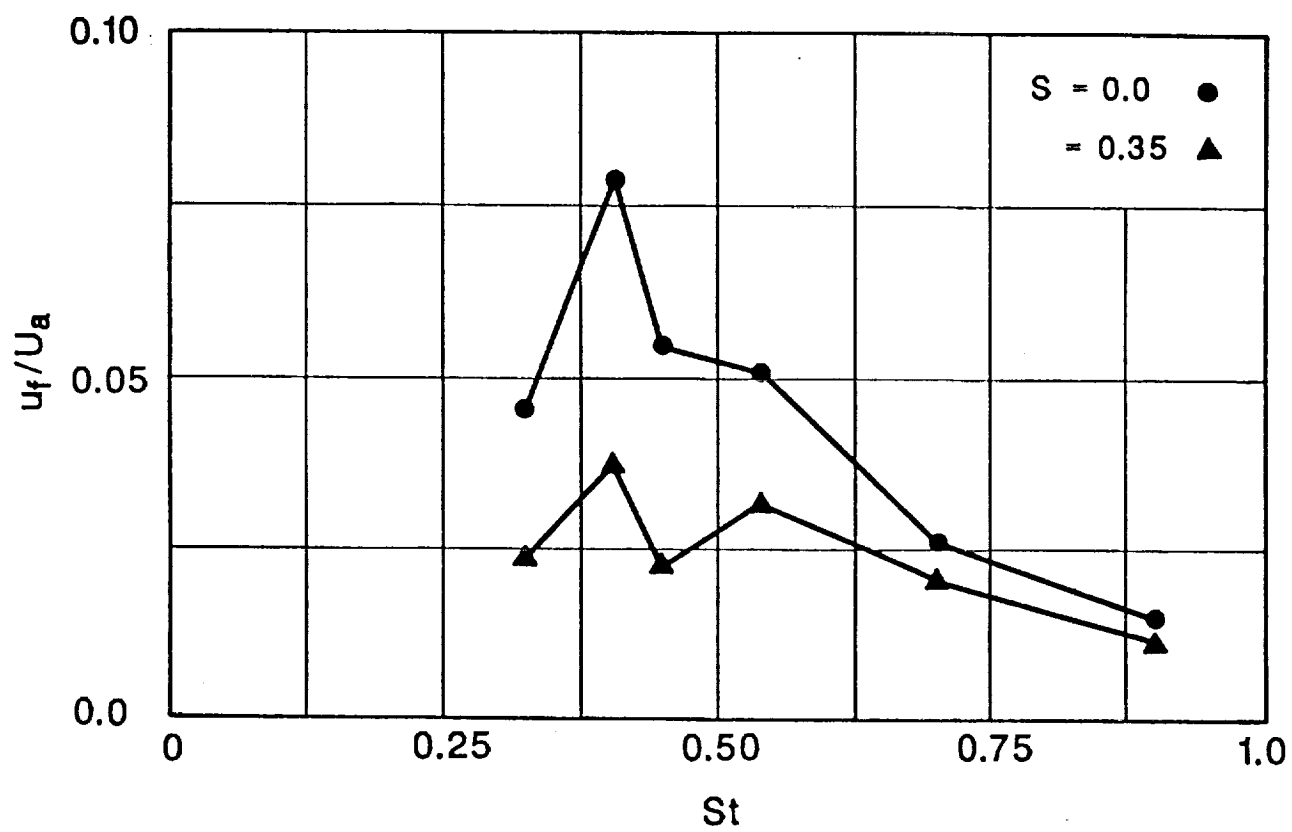
Fig. 11 Variation of peak (rms) amplitude of
the fundamental citation Strouhal number.
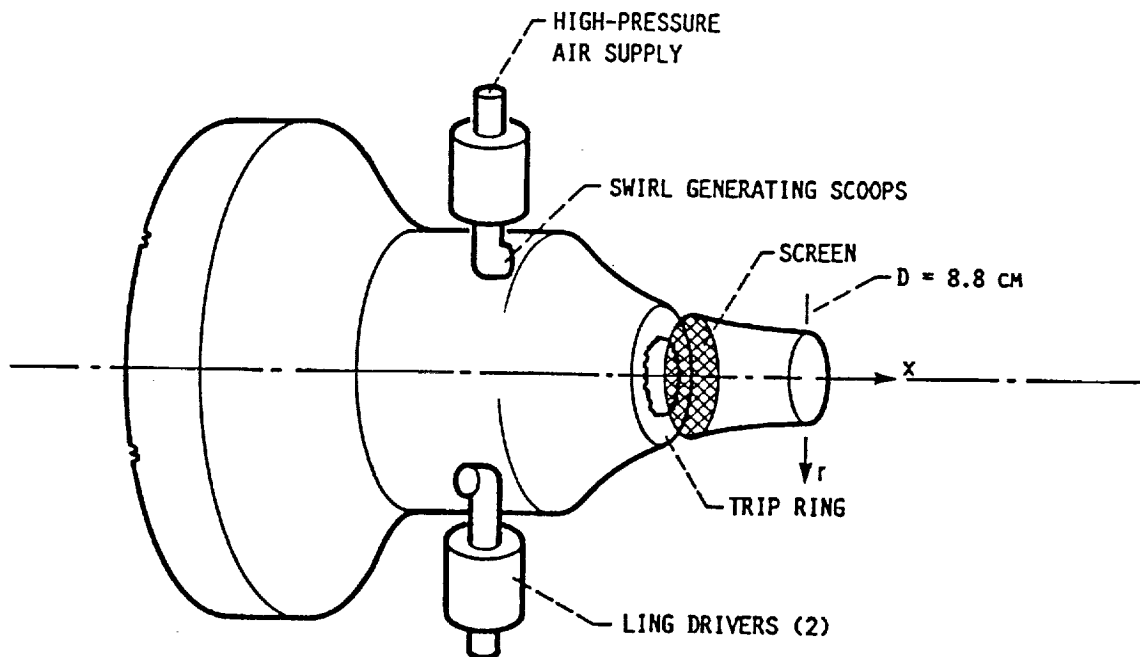
Fig. 12 Schematic of jet facility.
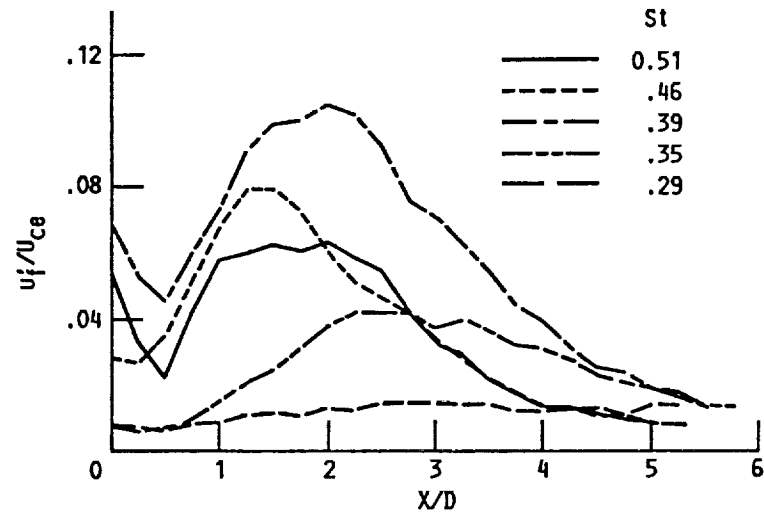
Fig. 13 Growth of the fundamental wave along the jet centerline. S = 0.12, M = 0.22.
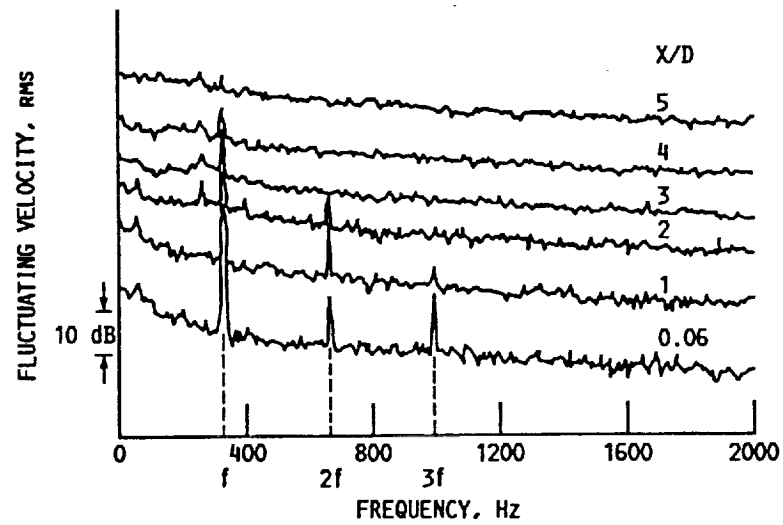
Fig. 14 Evolution of u'-spectra along the jet axis. St = 0.39, S = 0.12, M = 0.22, bandwidth = 7.5 Hz.

(a) RMS FLUCTUATIONS.

(b) MEAN.
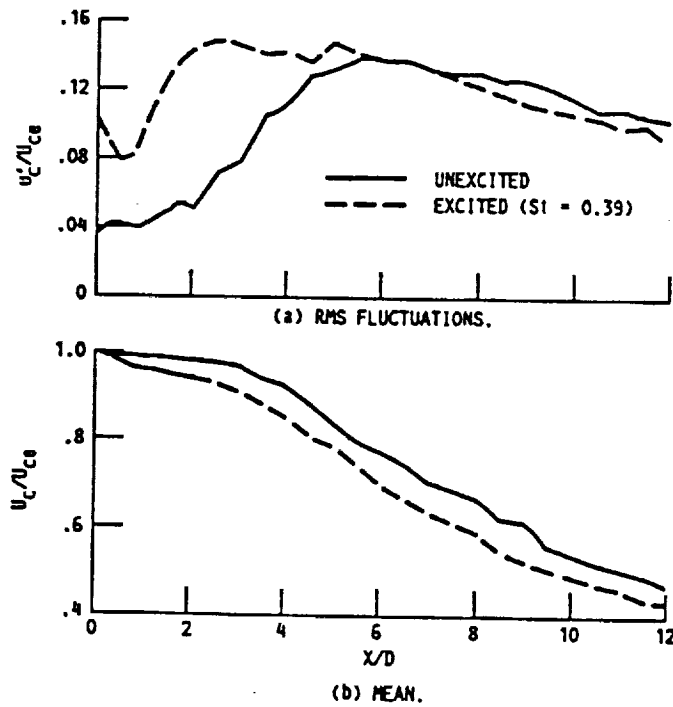
Fig. 15 Effect of excitation on the axial
velocity components along the jet axis.
S = 0.12, M = 0.22.
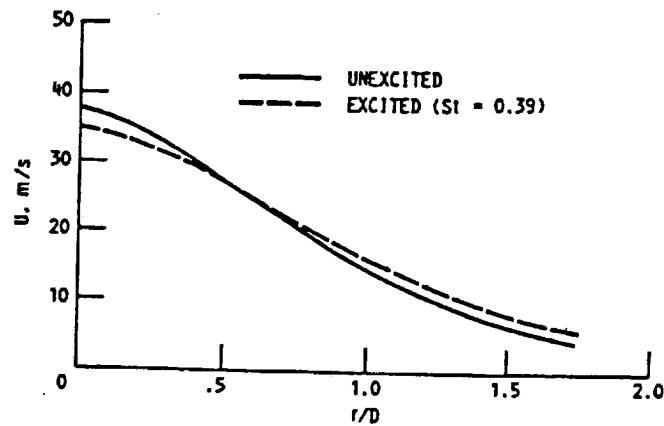
Fig. 16 Radial distributions of the time-mean
axial velocity at x/D = 7 with and
without excitation (S = 0.12).

39
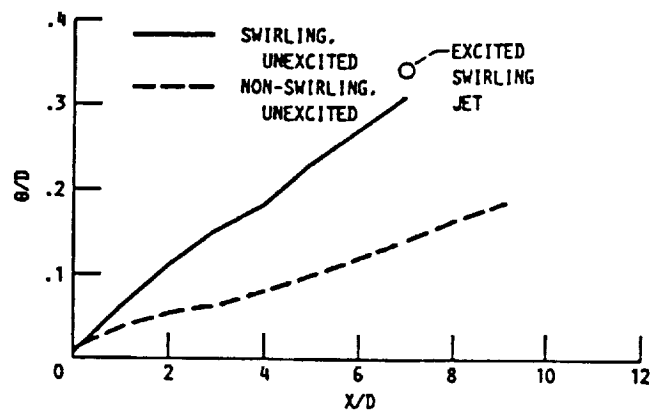
Fig. 17 Variation of momentum thickness along the jet axis.

(a) AXIAL.

(b) TANGENTIAL.
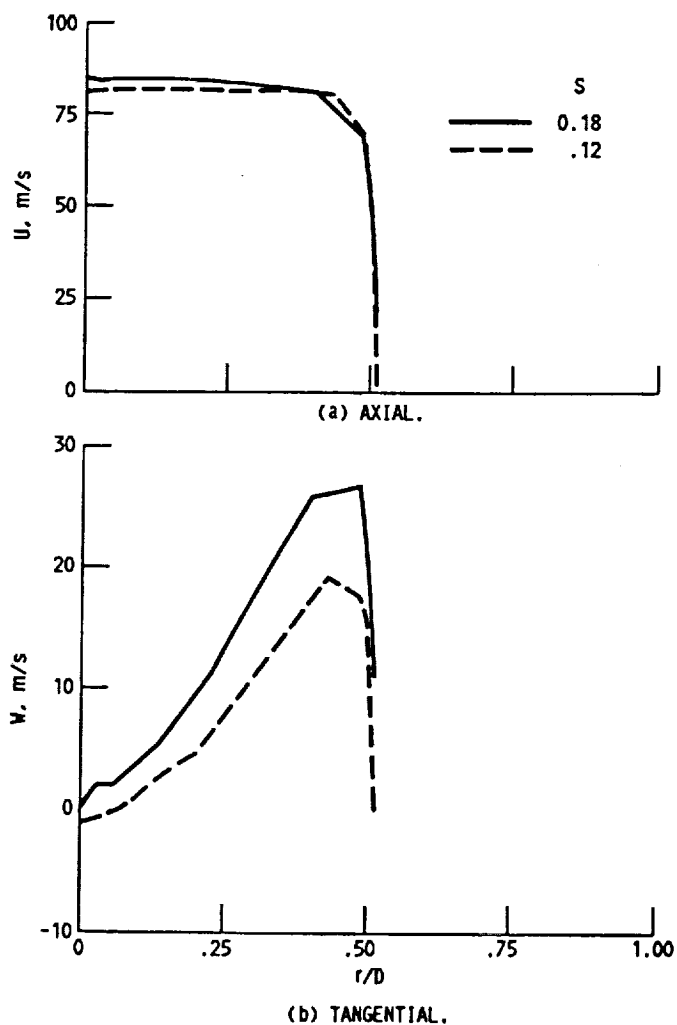
Fig. 18 Radial distributions of the time-mean velocity components at the nozzle exit at different swirl numbers.
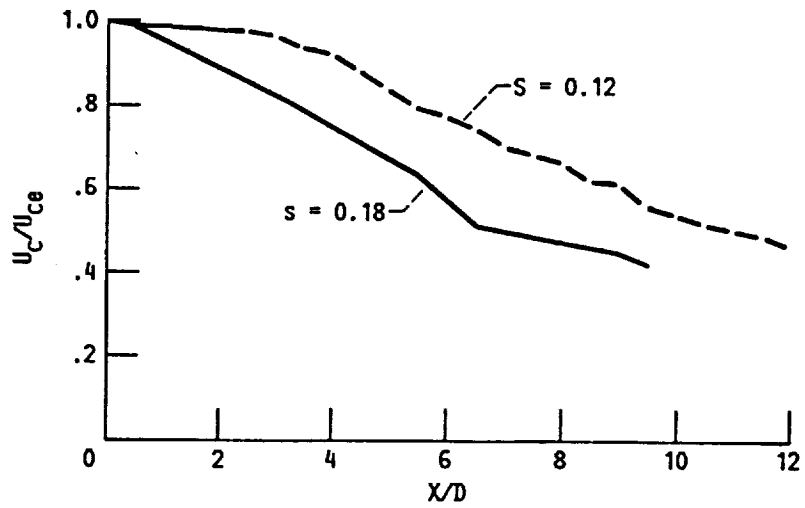
Fig. 19   Effect of swirl number on the downstream
          development of the time-mean axial velocity
          along the jet axis.   Unexcited.
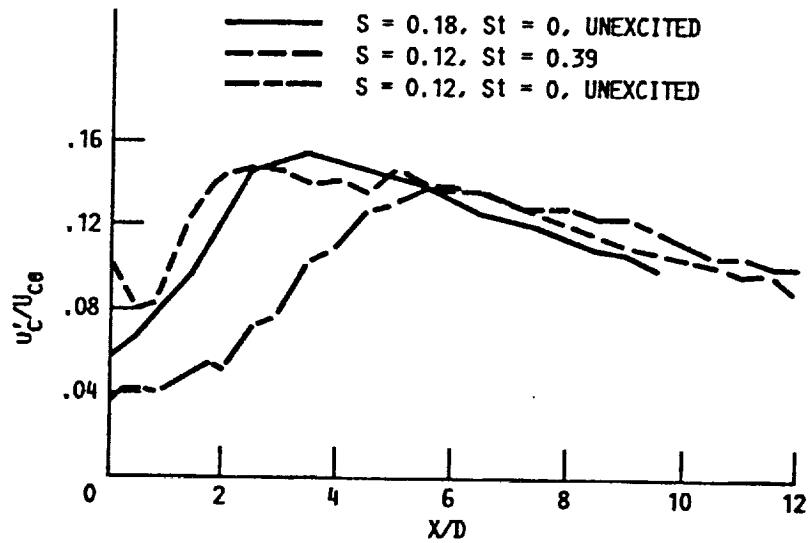

Fig. 20   Effect of swirl number and excitation
          on the distribution turbulence intensity
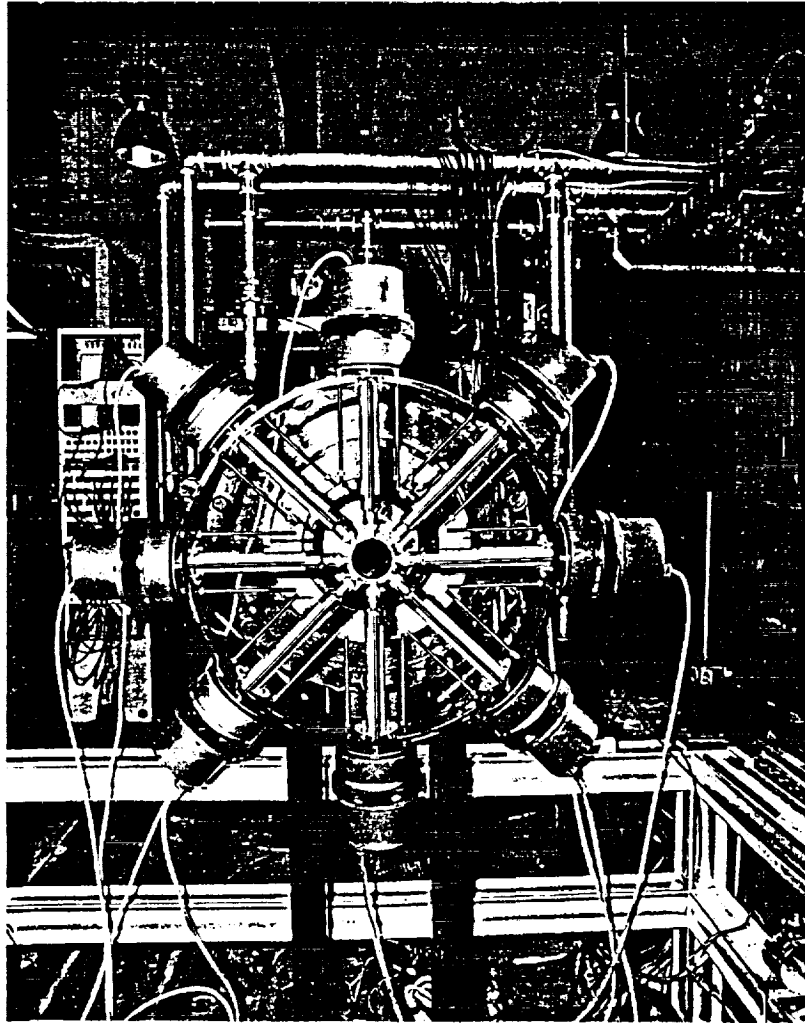   along the jet axis.

Fig. 21 Shear-layer control facility with
external excitation ring.